The ferroelastic phase transition in $(NH_4)_4LiH_3(SO_4)_4$: Brillouin scattering studies and Landau theory modeling

1993 J. Phys.: Condens. Matter 5 6377

(http://iopscience.iop.org/0953-8984/5/35/004)

J. Phys.: Condens. Matter 5 (1993) 6377–6386. Printed in the UK

The ferroelastic phase transition in $(NH_4)_4LiH_3(SO_4)_4$: Brillouin scattering studies and Landau theory modelling

B Mróz†, H Kiefte‡, M J Clouter‡ and J A Tuszyński§

† Institute of Physics, A Mickiewicz University, Grunwaldzka 6, 60-780 Poznań, Poland

‡ Department of Physics, Memorial University of Newfoundland, St John's, Newfoundland, AIB 3X7, Canada

§ Department of Physics, University of Alberta, Edmonton, Alberta, T6G 2J1, Canada

Received 28 April 1993

Abstract. High-resolution Brillouin spectroscopy was used to study the elastic properties of $(NH_4)_4LiH_3(SO_4)_4$ (ALHS). The temperature dependences of eleven Brillouin modes from acoustic phonons, propagating in the [100], [001], [110] and [101] directions, were measured in the temperature range from 140 to 300 K. The greatest elastic anomaly was observed in the plane perpendicular to the [001] crystallographic axes. The soft elastic constant c_{2S} was found to vanish at $T \simeq 232$ K. A Landau-type free-energy expansion is postulated and discussed, in order to explain the observed elastic anomalies.

1. Introduction

Among the ferroelastic crystals is a large group for which the appearance of the ferroelastic order parameter is related to the spatial ordering of BO_4 tetrahedra, where $BO_4 = SO_4$, SeO_4. A number of papers have been published on investigations of crystals with the general formula $A_4LiH_3(BO)_4$ where A = Rb, K, NH_4 and $BO_4 = SO_4$ or SeO_4 [1–10]. The best-known ferroelastic representative of this group is $Rb_4LiH_3(SO_4)_4$ [2,4,5,7]. Ferroelasticity has also been postulated in $Rb_4LiH_3(SeO_4)_4$ [11] and $Rb_4LiD_3(SO_4)_4$ [12]. All these materials undergo phase transitions from the high-temperature prototype symmetry $P4_1$ (point group 4) to the low-temperature elastic phase of monoclinic symmetry $P2_1$ (point group 2) at 131, 101 and 102 K, respectively.

Recently, it was suggested from x-ray studies and domain structure observations that $(NH_4)_4LiH_3(SO_4)_4$ and $(NH_4)_4LiH_3(SO_4)_4$ exhibit the same phase sequence with ferroelastic phase transitions at about 233 and 266 K, respectively [13]. The ferroelastic character of the phase transition in $(NH_4)_4LiH_3(SO_4)_4$ (abbreviated henceforth as ALHS) was confirmed by studies of the thermal and elastic properties [14]. The elastic properties of ALHS were studied using the torsion vibration technique. Combinations of the elastic stiffness tensor components coupled to the strains in the plane perpendicular to the [001] crystallographic direction were found to be strongly temperature dependent on both sides of the transition, exhibiting a distinct softening. Using these results, together with the results of DTA and thermal expansion studies, it was concluded that ALHS undergoes a continuous ferroelastic phase transition from the tetragonal point group 4 to the monoclinic 2 at about 235 K.

In this paper, we report high-resolution Brillouin scattering studies of ALHS crystals in the temperature range from 140 to 300 K. We have measured the temperature dependence of eleven Brillouin modes from the acoustic phonons propagating in the [100], [001], [110]

0953-8984/93/356377+10$07.50

and [101] directions. The results allowed us to calculate all non-zero components of the elastic stiffness tensor of the prototype phase 4.

In section 4, we present a phenomenological model of the phase transition studied. This model, based on the Landau expansion of the order parameter $\alpha(e_1 - e_2) + \beta e_6$, is compared to the previously developed theoretical description of the ferroelastic phase transition of $Rb_4LiH_3(SO_4)_4$ [7].

2. Experimental procedure

Crystals of ALHS were grown isothermally at 315 K by the dynamic method from an acid aqueous solution (pH $\leqslant$ 1) of the appropriate initial salts close to stoichiometric proportions [15] in the Crystal Physics Division of the Institute of Physics, A Mickiewicz University, Poznań, Poland. Samples of four different orientations were prepared in the form of cubes ($5 \times 5 \times 5$ mm^3). We measured the sound velocities along the crystallographic axes and the bisectors of these axes.

The Brillouin spectrometer has previously [16] been described in detail. The incident light was provided by a stabilized single-mode argon-ion laser (INNOVA-90, Coherent) operating at 514.5 nm. The scattered light was analysed at 90° using a piezo-electrically-scanned triple-pass Fabry–Perot interferometer (Burleigh RC-110) with free spectral ranges (FSRs) of 28.14, 19.66 and 11.59 GHz. The finesse was better than 50 and the measured contrast ratio was about 10^6.

The spectra were accumulated with a photon-counting data acquisition and stabilization system (Burleigh, DAS-1). The sound velocities v were deduced from the measured frequency shifts $\Delta\nu$ using the Brillouin equation

$$v = \lambda\Delta\nu(n_i^2 + n_s^2 - 2n_i n_s \cos\theta)^{-1/2} \tag{2.1}$$

where λ is the wavelength of the incident light, n_i and n_s are refractive indices for the incident and scattered light, respectively, and θ is the scattering angle ($\theta = 90°$). The refractive indices for ALHS were found, using the microscopic method, to be $n_x = n_y = 1.52$ and $n_z = 1.52$. All measurements were performed in the temperature range from 140 to 300 K. The temperature of the sample was regulated with a stability of ± 0.03 K using the temperature controller (Lakeshore Crytronics, model DC-500). The typical collection time of a well defined spectrum was about 3 h.

Since ALHS crystals were found to be highly hygroscopic, the polishing, storing and measurements were done in a dry environment. To avoid damage to the polished surfaces of the samples, the cryostat was preheated about 15 K above the ambient temperature before loading the samples.

3. Experimental results

At room temperature, ALHS shows tetragonal symmetry $P4_1$ (point group 4) with $a = 7.642$ Å and $c = 29.566$ Å [11]. The elastic stiffness tenor of this point group contains seven independent components: c_{11}, c_{12}, c_{13}, c_{16}, c_{33}, c_{44} and c_{66}. The relations between these components and the sound velocities deduced from the Brillouin shifts were found from solutions of the equation of motion given by vanishing of the determinant:

$$|c_{ijkl}q_j q_k - \rho v^2 \delta_{il}| = 0 \tag{3.1}$$

where q_j, q_k are the direction cosines of the phonon, ρ is the density of the crystal and c_{ijkl} are elastic constants.

The density of ALHS was calculated from the x-ray data presented in [11] to be 1.795 g cm^{-3} at room temperature. Following from thermal expansion studies of this crystal [14], the temperature dependence of density can be neglected in our calculations.

Table 1 presents ρv^2 as a function of elastic constants for the pure longitudinal (L), pure transverse (T), quasilongitudinal (QL) and quasitransverse (QT) modes of the tetragonal paraelastic phase 4. The temperature dependences of the Brillouin shifts (as listed in table 1) of ALHS are presented in figure 1. From this figure it is evident that all the observed modes (except the transverse modes $\gamma_3 = \gamma_6 = \gamma_9$ related to the c_{44} elastic constant) are affected by the transition. For the 4 $\rightarrow$ 2 ferroelastic phase transition, the crystal lattice shows elastic instability in the plane perpendicular to the fourfold axis of the tetragonal system. The greatest elastic anomalies, in fact, were observed for the phonons propagating in the [100] $\equiv$ [010] and [110] directions.

Table 1. ρv^2 as a function of the elastic constants for the point group 4.

Phonon	Mode		ρv^2 for the tetragonal phase 4
[100] $\equiv$ [010]	γ_1	QL	$\frac{1}{2}\{c_{11}+c_{66}+[(c_{11}-c_{66})^2+4c_{16}^2]^{1/2}\}$
	γ_2	QT	$\frac{1}{2}\{c_{11}+c_{66}-[(c_{11}-c_{66})^2+4c_{16}^2]^{1/2}\}$
	γ_3	T	c_{44}
[001]	γ_4	L	c_{33}
	γ_5	T	c_{44}
	γ_6	T	c_{44}
[110]	γ_7	QL	$\frac{1}{2}\{c_{11}+c_{66}+[(c_{12}+c_{66})^2+4c_{16}^2]^{1/2}\}$
	γ_8	QT	$\frac{1}{2}\{c_{11}+c_{66}-[(c_{12}+c_{66})^2+4c_{16}^2]^{1/2}\}$
	γ_9	T	c_{44}
[101] $\equiv$ [011]	γ_{10}	QL	
	γ_{11}	QT	$\gamma^3 - A\gamma^2 + B\gamma - C = 0$
	γ_{12}	QT	

$A = \frac{1}{2}(c_{11}+c_{33}+3c_{44}+c_{66})$.
$B = \frac{1}{2}[(c_{11}+c_{44})(c_{33}+c_{44})+(c_{11}+c_{44})(c_{44}+c_{66})+(c_{44}+c_{66})(c_{33}+c_{44})-(c_{44}-c_{13})^2-c_{16}^2]$.
$C = \frac{1}{2}[(c_{11}+c_{44})(c_{44}+c_{66})(c_{33}+c_{44})-(c_{44}+c_{13})^2(c_{44}+c_{66})-c_{16}^2(c_{33}+c_{44})]$.

Table 2. Elastic constants of ALHS at 295 K (in units of 10^{10} N m^{-2}).

c_{11}	c_{33}	c_{44}	c_{66}	c_{12}	c_{13}	c_{16}
2.56 ± 0.03	3.41 ± 0.04	0.56 ± 0.02	0.69 ± 0.03	1.98 ± 0.06	2.17 ± 0.06	0.28 ± 0.05

The frequency of the longitudinal γ_1 mode linearly decreases with lowering temperature and then rapidly increases from 15.68 GHz at T_c to 18.14 GHz at 141.2 K. The transverse mode γ_2 exhibits only a slight softening at T_c (figure 1(a)). The temperature dependence of the γ_4 longitudinal mode is presented in figure 1(b). The frequency of this mode increases linearly with decreasing temperature and shows a slight change of slope at T_c.

In figure 1(c), we present the temperature dependence of frequencies of the longitudinal γ_7 and transverse γ_8 modes. The frequency of the γ_7 mode increases with decreasing

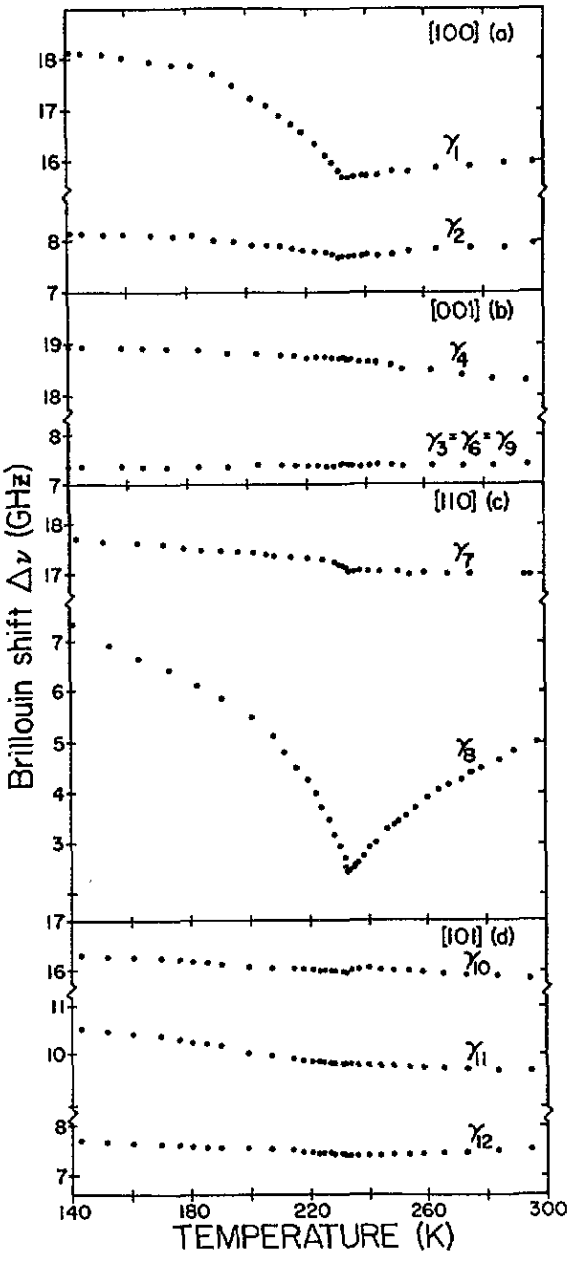

Figure 1. Temperature dependence of Brillouin frequency shifts for phonons propagating in the directions (*a*) [100], (*b*) [001], (*c*) [110], and (*d*) [101] in ALHS.

temperature, showing a slight anomaly at about 232 K. The strongest temperature dependence of the Brillouin shift was observed for the γ_8 mode. Its frequency falls from 5.02 GHz at room temperature to 2.41 GHz at T_c(= 232.2 K) and then rapidly increases to reach 7.34 GHz at 140.6 K. To define the character of the observed anomaly,

we have checked the temperature dependence of the squared frequency of the γ_8 mode on the both sides of the transition. We found that $(\Delta\nu)^2$ obeys the Curie–Weiss law in the entire temperature range studied for the paraelastic phase to about 30 K below T_c. The temperature dependence of $(\Delta\nu)^2$ for the paraelastic and ferroelastic phases can be described as $(\Delta\nu)^2 = 0.304(T - T_c) + 6.25$ and $(\Delta\nu)^2 = 0.801(T_c - T) + 6.35$, respectively (in units of GHz^2). Finally, in figure 1(*d*) we have plotted the temperature dependence of the frequencies γ_{10} (QL), γ_{11} (QT) and γ_{12} (QT) modes. As is evident, all these modes are only slightly affected by the transition.

The temperature dependences of ρv^2 for all the observed modes are plotted in figure 2. For the tetragonal phase 4, the simple relation $\rho v^2 = c_{ij}$ is valid only for $\gamma_4(\rho v^2 = c_{33})$ and $\gamma_3 = \gamma_6 = \gamma_9$ $(\rho v^2 = c_{44})$. The ρv^2 values of the remaining modes are given by the combinations of the non-zero components of the elastic stiffness tensor of the point group 4. The velocity of the most temperature-dependent mode γ_8 falls from 1203 m s^{-1} at 295 K to 578 m s^{-1} at T_c. The results presented in figure 2 allowed us to calculate all elastic constants of the prototype phase. Table 2 contains the room-temperature values of the elastic constants of the tetragonal high-temperature phase.

According to the group theory approach, for phase transformations involving the elastic instabilities of the crystal lattice [17], a transition of $4 \rightarrow 2$ type is accompanied by the onset of spontaneous strain $\alpha(e_1 - e_2) + \beta e_6$ below T_c and with the softening of the elastic constant:

$$c_{2S} = \tfrac{1}{2}\{c_{11} - c_{12} + c_{66} - [(c_{11} - c_{12} + c_{66})^2 + 8c_{16}^2]^{1/2}\}. \tag{3.2}$$

In order to determine the temperature dependence of the soft elastic constant, we have calculated [18] the temperature dependence of the elastic constants appearing in equation (3.2). Figure 3 shows the temperature dependence of the c_{11}, c_{12}, c_{66} and c_{16} elastic constants in the temperature range covering both high- and low-temperature phases. The broken curves below T_c are used to emphasize that the calculation, without distinguishing c_{11} from c_{22} or c_{23}, may be done under the assumption of slight monoclinicity for phase 2. As is evident from figure 3, none of the plotted elastic constants are critically temperature dependent; their combination, however, given by the soft elastic constant c_{2S}, reaches zero for $T = T_c$ within experimental error (see figure 4). Close to the transition point, the temperature dependence of c_{2S} can be described as $c_{2S}^{p} = 4.4 \times 10^{-3}(T - T_c)$ and $c_{2S}^{f} = 16.7 \times 10^{-3}(T_c - T)$, in units of 10^{10} N m^{-2} (where superscripts p and f stand for para- and ferroelastic phases, respectively). Such temperature behaviour observed for ALHS differs from the corresponding changes of c_{2S} observed for $Rb_4LiH_3(SO_4)_4$ where the value of the soft elastic constant was found to be not equal to zero at T_c.

Finally, we discuss the correlation between the anisotropy of the sound velocity in the xy plane and the domain wall pattern. The $4 \rightarrow 2$ type ferroelastic transition is caused by the instability of the transverse wave for which the propagating direction is governed by the values of elastic constants c_{11}, c_{12}, c_{16} and c_{66} in the plane (001) the angular dependence of the sound velocity of this mode is given by the following equation [19, 20]:

$$2\rho v^2 = c_{11} - c_{66} - \{[(c_{11} - c_{66})\cos 2\theta + 2c_{16}\sin 2\theta]^2 + [4c_{16}\cos 2\theta + 2(c_{12} + c_{16})\sin 2\theta]^2\}^{1/2} \tag{3.3}$$

where θ is the angle of minimum velocity with respect to the [100] direction. In figure 5, we present the angular dependence of ρv^2 of the transverse mode calculated at 295 K and at T_c. Minimization of equation (3.3) with respect to θ gives

$$\tan(4\theta_{min}) = 4c_{16}/(c_{11} - c_{12} - 2c_{66}). \tag{3.4}$$

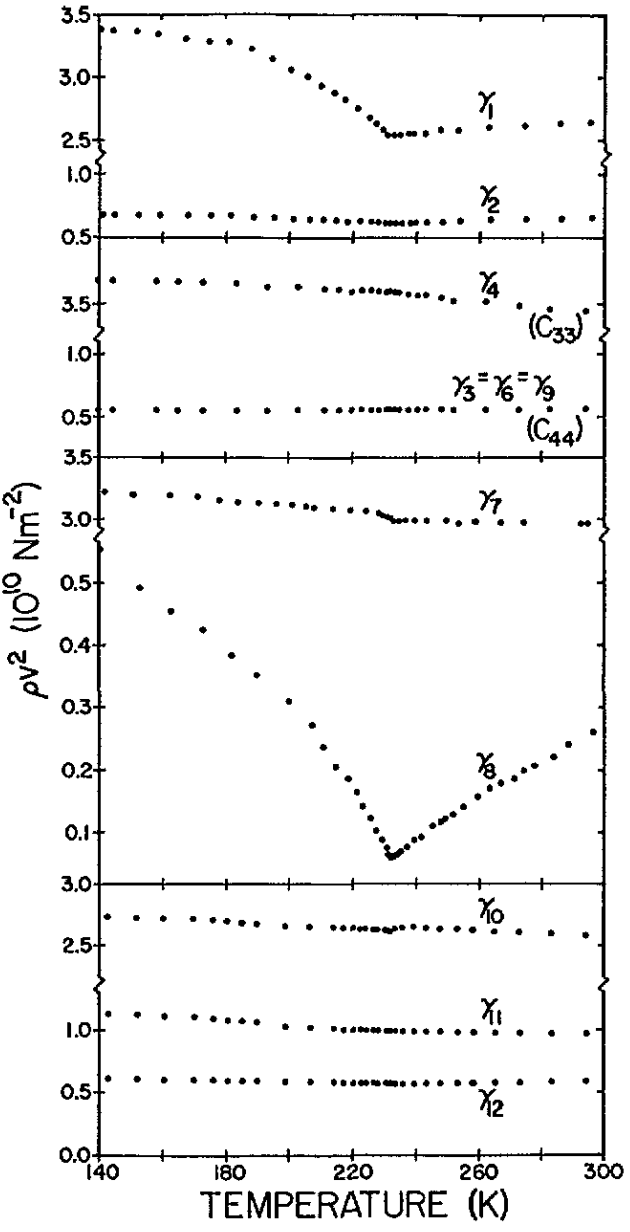

Figure 2. Temperature dependence of ρv^2 as determined from the data in figure 1.

The value of θ_{min} was found to be 31.5° and 33.5° at 295 K and T_c, respectively. The latter value of θ determines the expected orientation of domain walls close to the phase transition [21]. The domain walls forming at the $4 \rightarrow 2$ transition are of W' type [22] and their orientation depends on the components of the spontaneous strain tensors, which, in turn, are related to the elastic constant appearing in the expression for c_{2S}. A more detailed analysis of this problem will be presented in the near future.

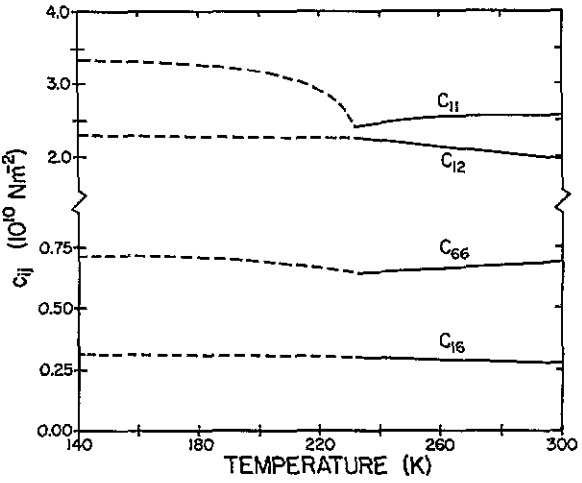

Figure 3. Temperature dependence of c_{11}, c_{12}, c_{16} and c_{66} elastic constants of ALHS.

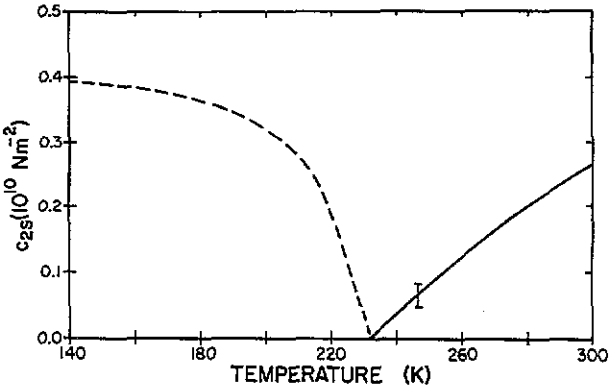

Figure 4. Temperature dependence of soft elastic constant c_{2S} calculated from equation (3.2). The error bar represents the estimated uncertainty.

4. Theoretical model

As argued above, we believe that the transition observed is of $4 \rightarrow 2$ type and is of second order. Following Boccara [17], we identify the spontaneous strain e_s as

$$e_s = \alpha(e_1 - e_2) + \beta e_6. \tag{4.1}$$

In the absence of strong evidence that coupling to other modes is involved, especially to dielectric polarization, we adopt a Landau free-energy expansion in the form

$$F = F_1(e_s) + F_2(\{e_i\}) \tag{4.2}$$

where e_i represents the remaining strain components. The question of the nature of $F_1(e_s)$ now arises. If we took the standard quartic expansion in terms of e_s, the corresponding soft elastic constant c_{2S} defined as

$$c_{2S} \equiv \mathrm{d}^2F/\mathrm{d}e_s^2 \tag{4.3}$$

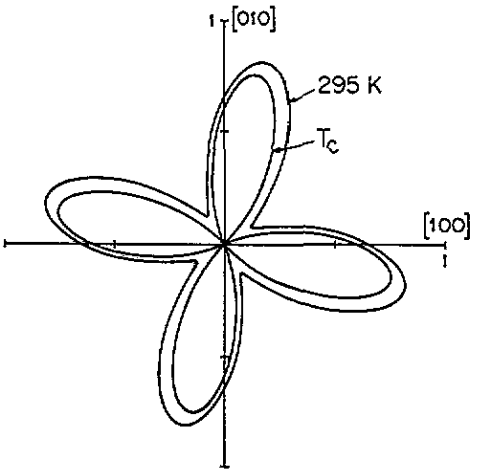

Figure 5. The angular dependence of ρv^2 calculated for the transverse mode in the plane (001) at 295 K and T_c (in units of 10^{10} N m^{-2}).

would be a linear function of temperature both above and below the critical temperature T_c. This is, however, not the case in our system as can be seen from figure 4. Then, for $T > T_c$ the plot of the elastic constant c_{2S} is quite linear but below T_c the plot of c_{2S} is strongly curved as a function of temperature. In order to model this behaviour, it is sufficient that we expand

$$F_1(e_s) = c_2 e_s^2 + c_4 e_s^4 + c_6 e_s^6 \tag{4.4}$$

where $c_2 = \alpha(T - T_c)$; $c_4 > 0$ and $c_6 > 0$. This ensures that the transition is second order and, as will be demonstrated later, also leads to qualitatively correct behaviour of c_{2S} both above and below T_c.

The remaining part of the free energy contains bilinear contributions from the allowed strained components, i.e. we take

$$F_2(\{e_i\}) = \sum_{ij} c_{ij}^{\circ} e_i e_j. \tag{4.5}$$

We now calculate the critical properties of the system based on the expansion in (4.4). Minimizing it with respect to e_s yields

$$0 = \mathrm{d}F_1/\mathrm{d}e_s = 2c_2 e_s + 4c_4 e_s^3 + 6c_6 e_s^5. \tag{4.6}$$

Above T_c this is solved by $e_s = 0$ while below T_c a non-zero value of the order parameter is found, namely

$$e_s^2 = \left(-4c_4 + \sqrt{16c_4^2 - 48c_2c_6}\right) \Big/ 12c_6 \tag{4.7}$$

where we have discarded the $-$ sign in front of the square root which applies to first-order phase transitions and hence to the case with $c_4 < 0$. Calculating c_{2S} according to (4.3) and inserting (4.7) yields its temperature dependence below T_c as

$$c_{2S} = -8\alpha(T - T_c) + \tfrac{8}{3}(c_4^2/c_6)\left[1 - \sqrt{1 - 3\alpha(T - T_c)c_6/c_4^2}\right]. \tag{4.8}$$

Note that at $T = T_c$, $c_{2S} = 0$, signalling complete mode softening, as observed in our experiment. Close to T_c, the square root in (4.8) can be expanded in a Taylor series which gives

$$c_{2S} = -4\alpha(T - T_c) + (3c_6\alpha^2/c_4^2)(T - T_c)^2 + \cdots \tag{4.9}$$

with the desired quadratic contribution to c_{2S} (T) below T_c. Above T_c where $e_s = 0$ we find from (4.3) and (4.4) that

$$c_{2S} = 2\alpha(T - T_c) \qquad (T > T_c). \tag{4.10}$$

(4.10) is consistent with the Curie–Weiss law mentioned in the experimental part of the paper since the inverse susceptibility function χ for $T > T_c$ is equal to c_{2S}. Furthermore, from the data presented in section 3 we readily find that $\alpha = 2.2 \times 10^{-3}$ in units of 10^{10} N m^{-2}.

Thus, both (4.9) for $T < T_c$ and (4.10) for $T > T_c$ are consistent with experimental observations (see figure 4).

The remaining elastic constants are calculated according to

$$c_{ij} = \partial^2 F/\partial e_i \partial e_j. \tag{4.11}$$

In particular, for c_{11} and c_{66} we obtain

$$c_{11} = c_{11}^\circ + \alpha^2 c_{2S} \tag{4.12}$$

and

$$c_{66} = c_{66}^\circ + \beta^2 c_{2S}. \tag{4.13}$$

The presence of non-critical contributions c_{11}° and c_{66}° explains the observed lack of complete softening of these two modes. Furthermore, from the experimental plots of c_{11} and c_{66} in figure 3 we can calculate the respective contributions of $(e_1 - e_2)$ and e_6 towards the order parameter e_s. We thus find that $\alpha/\beta \simeq 4.0$. This has been calculated by first finding the values of $c_{11}(T_c)$, $c_{11}(T = 140\ \text{K})$ and $c_{66}(T_c)$, $c_{66}(T = 140\ \text{K})$, followed by an estimate of $[c_{11}(T = 140\ \text{K}) - c_{11}(T_c)]/[c_{66}(T = 140\ \text{K}) - c_{66}(T_c)]$. This latter expression, when the square root is taken, gives the value of α/β.

We conclude that a simple Landau expansion involving the order parameters to sixth order and the remaining elastic constants bilinearly provides a consistent theoretical description of the experimental data.

References

[1] Krajewski T, Bręczewski T, Piskunowicz P and Mróz B 1988 *Proc. 8th Czechoslovak–Polish Seminar on Structural and Ferroelastic Phase Transitions (Senohraby, 1988)*

[2] Połomska M and Smutný F 1988 *Phys. Status Solidi* b **154** K103

[3] Minge J and Krajewski T 1988 *Phys. Status Solidi* a **109** 193

[4] Wołejko T, Pakulski G and Tylczyński Z 1988 *Ferroelectrics* **81** 1979

[5] Piskunowicz P, Bręczewski T and Wołejko T 1989 *Phys. Status Solidi* a **114** 505

[6] Mróz B and Laiho R 1989 *Phys. Status Solidi* a **115** 575

[7] Mróz B, Kiefte H, Clouter M J and Tuszyński J A 1991 *J. Phys.: Condens. Matter* **3** 5673

[8] Pietraszko A and Łukaszewicz K 1988 *Z. Krystallogr.* **185** 564

[9] Zunina F J, Extebarria G, Madariaga G and Bręczewski T 1990 *Acta Crystallogr.* C **46** 1199

[10] Mróz B, Kaczmarski M, Kiefte H and Clouter M J 1992 *J. Phys.: Condens. Matter* **4** 7515
[11] Pietraszko A, Połomska M and Pawłowski A 1991 *Izv. Akad. Nauk Ser. Fiz.* **55** 529
[12] Przesławski J, Glazer A M and Czapla Z 1990 *Solid State Commun.* **74** 1165
[13] Połomska M, Pawłowski A, Smutný F and Wolak J 1992 *2nd Int. Symp. on Domain Structure of Ferroelectrics and Related Materials (Nantes)*
[14] Mróz B, Piskunowicz P, Pawłowski A and Krajewski T 1993 *8th Int. Meeting on Ferroelectricity* (Gaithersburg, MD: NIST)
[15] Pawłowski A 1993 personal communication
[16] Mróz B, Kiefte H, Clouter M J and Tuszyński J A 1992 *Phys. Rev.* B **46** 8717
[17] Boccara N 1964 *Ann. Phys., NY* **47** 40
[18] Brose K H 1989 *ELCON A Computer Program for Fitting Constants to Phonon Velocities* (Detroit: Wayne State University Press)
[19] 1963 *American Institute of Physics Handbook* (New York: McGraw-Hill)
[20] Every A G 1980 *Phys. Rev.* B **22** 1746
[21] Cho M, Yagi T, Fuji T, Sawada A and Ishibashi Y 1982 *J. Phys. Soc. Japan* **51** 2914
[22] Sapriel J 1975 *Phys. Rev.* B **12** 5128